Conference Proceedings of the Society for Experimental Mechanics Series

Evro Wee Sit *Editor*

Sensors and Instrumentation, Volume 5

Proceedings of the 34th IMAC, A Conference and Exposition on Structural Dynamics 2016

Springer

Conference Proceedings of the Society for Experimental Mechanics Series

Series Editor
Kristin B. Zimmerman, Ph.D.
Society for Experimental Mechanics, Inc.,
Bethel, CT, USA

More information about this series at http://www.springer.com/series/8922

Evro Wee Sit
Editor

Sensors and Instrumentation, Volume 5

Proceedings of the 34th IMAC, A Conference and Exposition on Structural Dynamics 2016

Springer

Editor
Evro Wee Sit
SVcommunity.com
Hermosa Beach, CA, USA

ISSN 2191-5644 ISSN 2191-5652 (electronic)
Conference Proceedings of the Society for Experimental Mechanics Series
ISBN 978-3-319-29858-0 ISBN 978-3-319-29859-7 (eBook)
DOI 10.1007/978-3-319-29859-7

Library of Congress Control Number: 2016940977

Printed on acid-free paper

This Springer imprint is published by Springer Nature
The registered company is Springer International Publishing AG Switzerland

Preface

Sensors and Instrumentation represents one of ten volumes of technical papers presented at the 34th IMAC, A Conference and Exposition on Structural Dynamics, organized by the Society for Experimental Mechanics, and held in Orlando, Florida, on January 25–28, 2016. The full proceedings also include volumes on Nonlinear Dynamics; Dynamics of Civil Structures; Model Validation and Uncertainty Quantification; Dynamics of Coupled Structures; Special Topics in Structural Dynamics; Structural Health Monitoring, Damage Detection & Mechatronics; Rotating Machinery, Hybrid Test Methods, Vibro-Acoustics and Laser Vibrometry; Shock & Vibration, Aircraft/Aerospace, Energy Harvesting, Acoustics & Optics; and Topics in Modal Analysis & Testing.

Each collection presents early findings from experimental and computational investigations on an important area within Sensors and Instrumentation. Topics represent papers on calibration, smart sensors, rotational effects, stress sensing, and tracking of dynamics.

The organizers would like to thank the authors, presenters, session organizers, and session chairs for their participation in this track.

Hermosa Beach, CA, USA — Evro Wee Sit

Contents

Chapter 1
Phase Control of RF Cavities

Brian Page, Orlando Murray, Patricia Tan, Alexandria N. Marchi, Alexander Scheinker, Daniel Rees, and Charles Farrar

Abstract Particle accelerators use superconducting radio frequency (RF) cavities that create extremely large electromagnetic fields to accelerate charged particles. The latest accelerators require an unprecedented level of precision in terms of particle energy, which translates into accelerating field amplitude and phase within error bounds of 0.01 % and 0.01°, respectively. To save money, it is possible to split the output of one high power controlled RF source to multiple cavities. However, in practice, all cavities are slightly different and experience different disturbances in operation. Because of an inability to quickly modulate the phase and amplitude of the individual split high power RF signals, the fields of an entire multi-cavity system are averaged and treated as one entity on which feedback control is performed at the low power input to the high power RF amplifier. The issue is compounded by the severe electrical loading that the RF cavity experiences during operation. Radiation pressure causes Lorentz force detuning, which shifts each cavity's resonance peak, amplitude, and phase of its accelerating field in a unique way. Piezo tuners have been used to counteract Lorentz force detuning of individual cavities. This paper studies RF cavity phase control via piezo tuners. The controller designed is capable of quickly modifying the natural frequency of a cavity as a tool for modulating the phase of an RF signal. The approach is validated in hardware with a Niobium coated single-cell copper TESLA-type RF cavity.

Keywords Particle accelerator • RF resonator • Resonance control • Lorenz force detuning • Phase shifting

1.1 Introduction

Radio frequency (RF) cavities are used in particle accelerators to generate acceleration gradients on the order of 20 MV/m. RF cavities operate by resonating electromagnetic fields at very high frequencies ranging from high MHz to low GHz. In an effort to lower costs, new accelerators are being designed with many clustered RF cavities that are fed by single high power klystrons, as shown in Fig. 1.1. Legacy control methods focus on averaging the phases and amplitudes of the entire bank of cavities and controlling the klystron output as well as using piezo tuners to counteract the dynamic Lorentz force detuning that occurs within each cavity at operational voltages [1–5]. For example, the Matter-Radiation Interactions in Extremes (MaRIE) experimental facility at Los Alamos National Laboratory plans to employ resonance cavities operating at approximately 1.3 GHz and 20 MV/m average acceleration gradient with 8–24 cavities driven by a single klystron. Each MaRIE accelerating cavity must be tuned to account for manufacturing variability and dynamic detuning during operation with an unprecedented degree of accuracy, i.e., amplitude and phase error bounds within 0.01 % and 0.01°, respectively.

B. Page
Department of Mechanical Engineering-Engineering Mechanics, Michigan Technological University, Houghton, MI 49931, USA

O. Murray
Department of Electrical and Computer Engineering, University of Florida, Gainesville, FL 32611, USA

P. Tan
Department of Structural Engineering, University of California, San Diego, La Jolla, CA 92093, USA

A.N. Marchi (✉) • C. Farrar
Los Alamos National Laboratory, Engineering Institute, MS T001, P.O. Box 1663, Los Alamos, NM 87545, USA
e-mail: amarchi@lanl.gov

A. Scheinker • D. Rees
Los Alamos National Laboratory, RF Engineering, MS T001, P.O. Box 1663, Los Alamos, NM 87545, USA

E. Wee Sit (ed.), *Sensors and Instrumentation, Volume 5*, Conference Proceedings of the Society for Experimental Mechanics Series, DOI 10.1007/978-3-319-29859-7_1

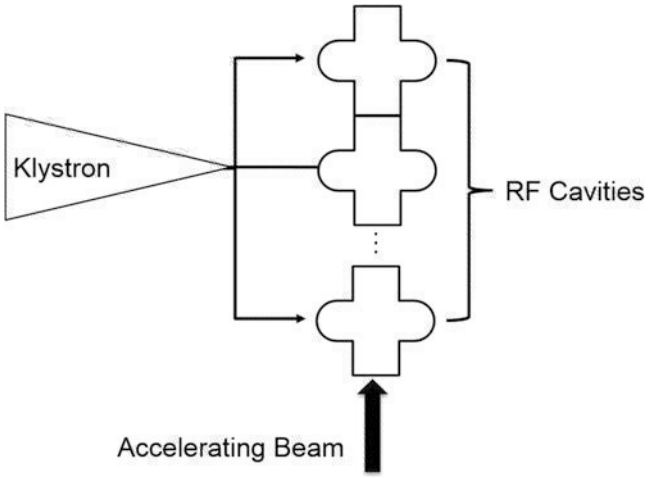

Fig. 1.1 Diagram of current accelerator layout

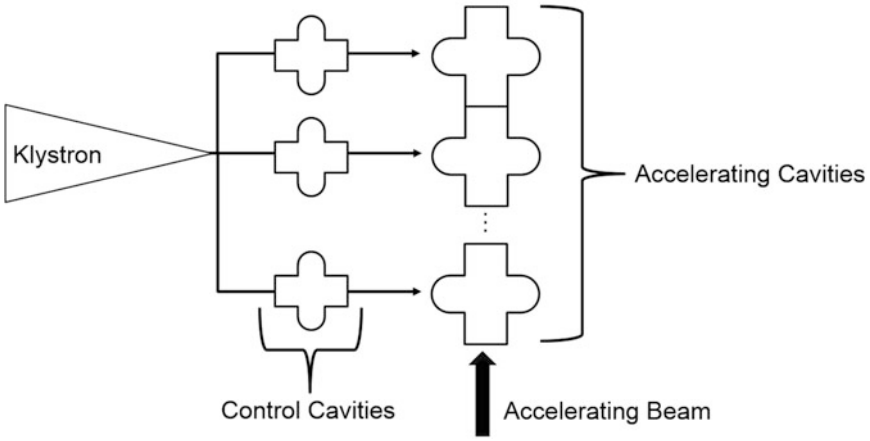

Fig. 1.2 Proposed accelerator with control cavities

This paper studies a new method for modulating high power RF signals. By placing additional RF cavities between the klystron and the accelerating cavities and using high power piezo-tuners the input phases and amplitudes of the RF fields entering each accelerating cavity may be modulated independently as shown in Fig. 1.2.

This method focuses on using multiple piezo tuners and individual feedback control loops for each control cavity. Through this method, it is possible to individually control the resonant frequency of each cavity in a bank of cavities through a relatively wide band of adjustments depending on the Q factor of the cavity and the piezo actuation. The control loop is a multilevel controller built around a low level PID feedback loop, and a high level synchronizer that ensures all the cavities operate together with the correct phase shift between cavities.

The designed low level PID loop operates on the IQ model of RF cavities in Eqs. (1.1) and (1.2). The IQ model separates the RF cavity into inphase (V_i) and quadrature (V_r) components of cavity voltage effectively separating the quickly oscillating RF signal from the relatively slow amplitude and phase shifting that occurs during operation. By using the IQ model, the control loop is able to operate at a much lower frequency and still effectively control the RF field.

$$\frac{dV_i}{dt} + \omega_{1/2} V_i - \Delta\omega V_r = \omega_{1/2} R_L I_i \tag{1.1}$$

$$\frac{dV_r}{dt} + \omega_{1/2} V_r - \Delta\omega V_i = \omega_{1/2} R_L I_r \tag{1.2}$$

In the IQ model, $\omega_{1/2}$ is the cavity bandwidth, $\Delta\omega$ is the difference between resonance frequency and input RF frequency, R_L is the cavity's resistance, and I is the driving current in both inphase and quadrature components.

1.2 Experimental Setup

Controller design is completed in both simulation and hardware. Simulations focus on the development of an IQ model of an RF cavity in Simulink while hardware validation is completed with LabVIEW on a Niobium coated single-cell copper TESLA-type RF cavity operating at approximately 1.3 GHz, shown in Fig. 1.3. Attached to the RF cavity are four piezo tuners, which are capable of modifying the length of the cavity and thus adjusting resonance. The cavity/piezo tuner assembly is mounted into a rigid frame. An RF antenna fed from a signal generator is used as the RF source for the cavity and another RF antenna acts as the receiver for the controller. The RF signal coming from the cavity is fed through a custom signal demodulator that converts the RF signal into amplitudes and phases that are relative to the input signal that results in steady state phase error bounds of $\pm 0.075°$. The cavity is used in non-superconducting mode but conclusions can be transferred to superconducting cavities.

Simulink modelling of the IQ model of an RF cavity is shown in Fig. 1.4. The model is built around the state space representation of the IQ model of RF cavities described in [6]. This model is capable of simulating both superconducting and non-superconducting through choice of the Q and R_L factors. In the model implemented Q was chosen to be 45,000 and R_L of 5 corresponding to a normal conducting cavity. The generic cavity model simulated allows for simulation of various controller and filtering strategies quickly.

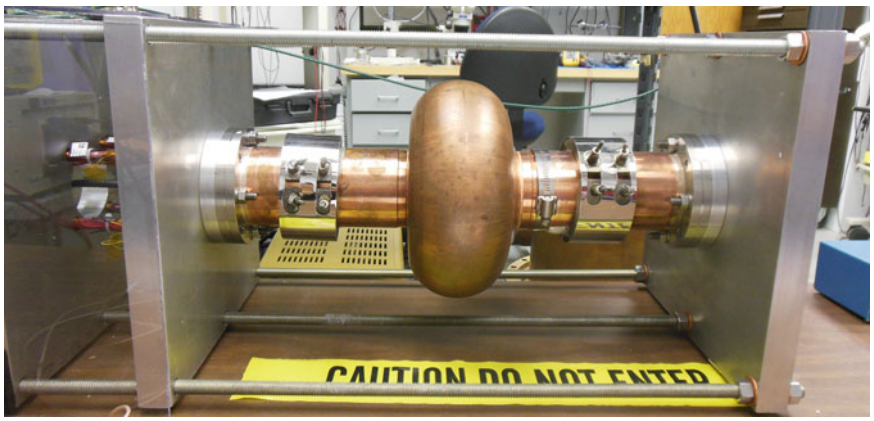

Fig. 1.3 TESLA-type RF cavity setup

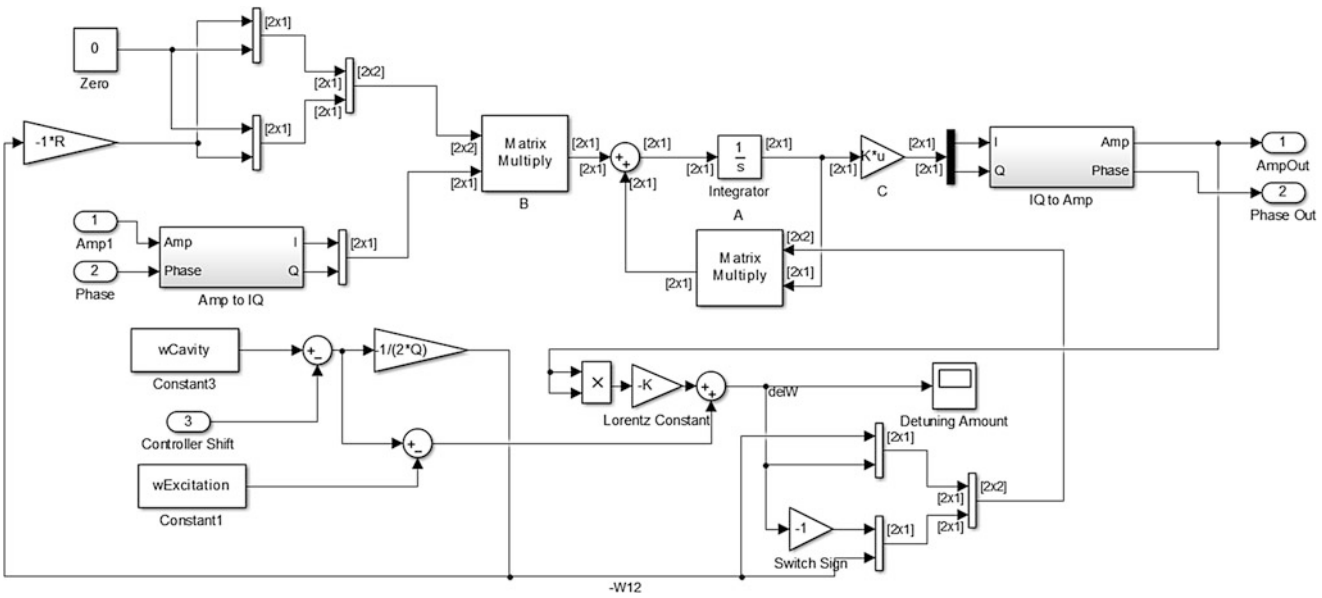

Fig. 1.4 State space model of RF cavity

Hardware validation of controller design is completed with National Instruments LabVIEW and a TESLA cavity. A closed loop control system is designed to guarantee performance of the cavity through the various detuning factors and across multiple cavities. Control tests focus around four possible use cases: (1) constant input frequency-constant target phase, (2) moving input frequency-constant target phase, (3) constant input frequency-moving target phase, and (4) moving input frequency-moving target phase.

1.3 Simulation Results

Controller development focuses on implementing a feedback system to control phase of the cavity output signal. Each RF cavity in a multi-cavity system is modeled as shown in Fig. 1.4, while the entire system is modeled together in Fig. 1.5. In the multi-cavity model, a standard PID controller is implemented based on the average of the output amplitudes in a similar fashion to legacy tuning methods. Phase is controlled by setting a constant target phase for the klystron and then using the control cavities (Red in Fig. 1.5) to dynamically shift the phase towards the target. This phase shifting is accomplished with PID control of the piezo actuation on the cavity walls. In simulation the control cavities are capable of shifting the phase $\pm 15°$in 160 ± 10 μs with a controller updating at 1 MHz. Provided powerful enough hardware, the fast phase shifting capabilities of RF cavities could be harnessed to shift phase within individual pulses or to maintain a constant phase in extremely noisy conditions.

1.4 Hardware Results

Hardware validation of simulation results is completed on a Niobium coated single-cell copper TESLA-type RF cavity using LabVIEW.

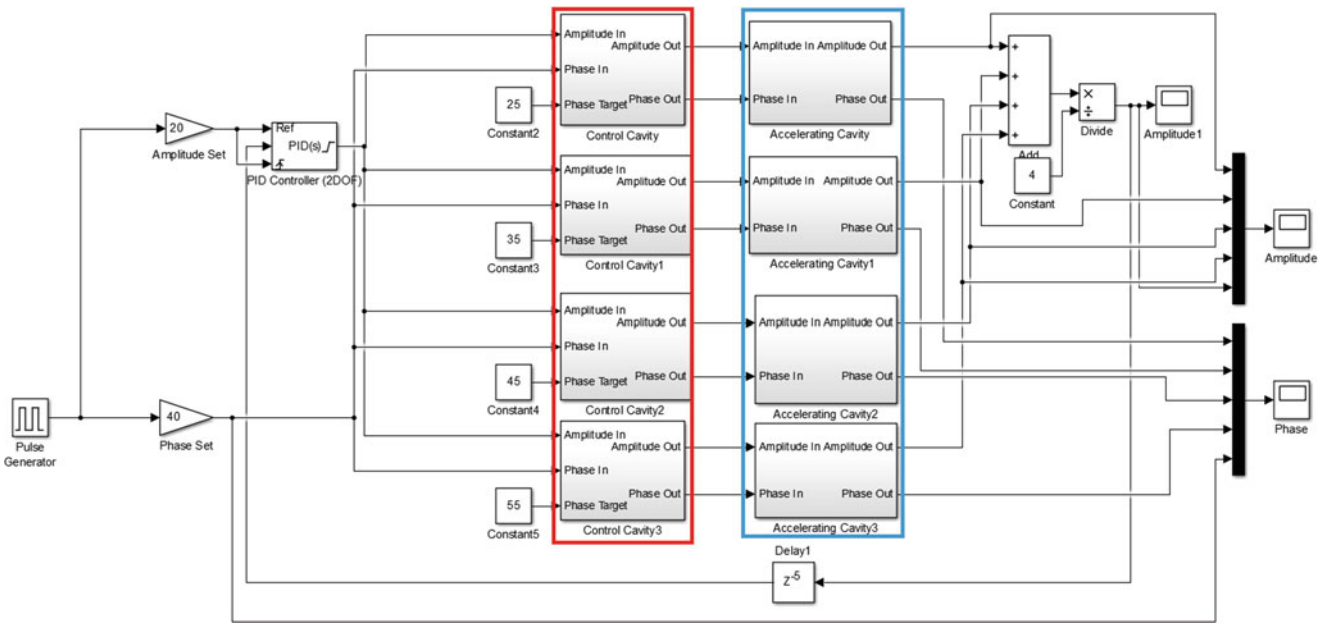

Fig. 1.5 Multicavity model of RF system

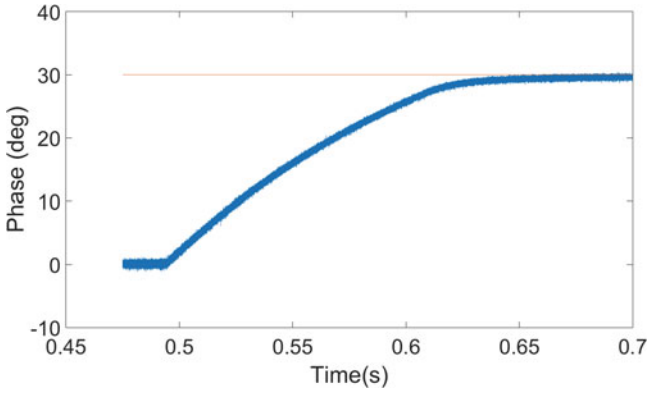

Fig. 1.6 Upper limit phase modulation

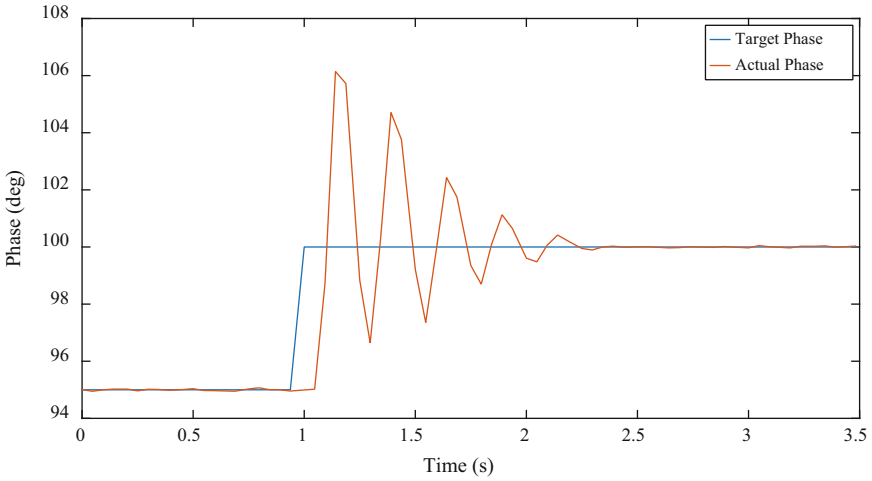

Fig. 1.7 Constant input frequency-constant target phase

1.4.1 Hardware Limitations

The piezo tuner/amplifier system is capable of shifting the resonance peak by approximately 200 kHz, which corresponds to a 30° phase swing in 0.15 s, shown in Fig. 1.6. This upper limit on phase swing and rate is determined by the capabilities of our amplifier. The 1 W amplifier reaches its current limit while charging the piezos, using a commercially available amplifier with 1 kW of output power, the 30° phase shift could be achieved in 150 μs.

A PID controller is developed in LabVIEW to control the piezo actuation against the phase error. The controller is able to operate at 20 Hz. This very slow control frequency could be improved to the point of functionality within the accelerator environment by using dedicated hardware, such as an FPGA. Four tests are completed to characterize the controller performance. These tests are (1) constant input frequency-constant target phase, (2) moving input frequency-constant target phase, (3) constant input frequency-moving target phase, and (4) moving input frequency-moving target phase.

1.4.2 Constant Input Frequency-Constant Target Phase

The constant input frequency-constant target phase test is the most likely use case in accelerator applications. This test involves inputting a constant frequency near the cavity resonance and tracking a step input for target phase as shown in Fig. 1.7. Shown here is a step input jumping from 95 to 100° phase shift. The controller is able to settle out this phase shift in 1.5 s to within 0.1° of the phase target. The signal demodulator accounts for much of the remaining phase error. After accounting for the demodulator error, the controller is accurate to within ±0.025° in this use case. With a faster control loop, settling time would be greatly reduced and accuracy improved.

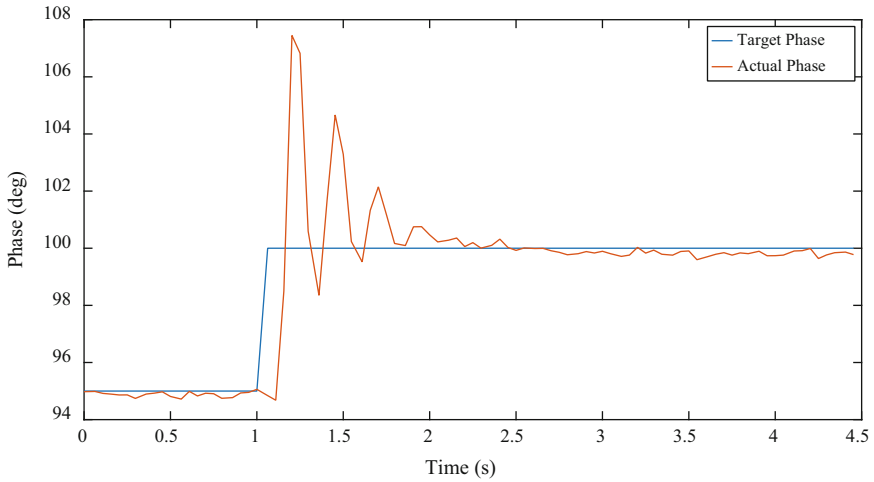

Fig. 1.8 Moving input frequency-constant target phase

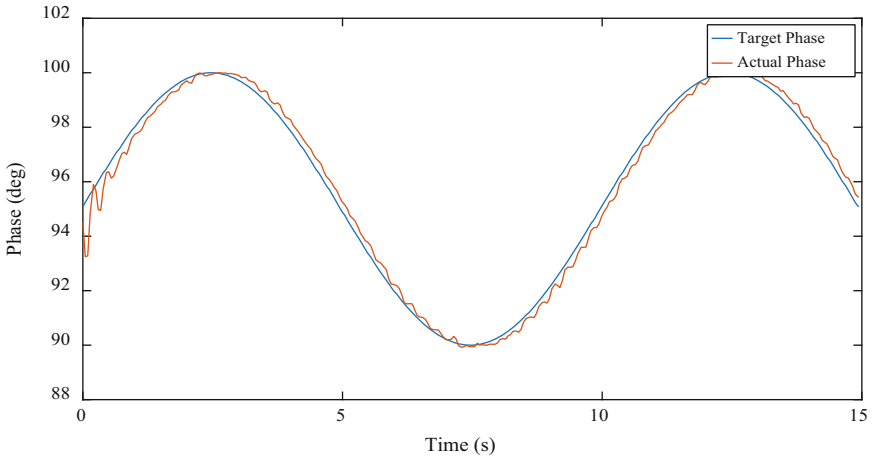

Fig. 1.9 Constant input frequency-moving target phase 0.1 Hz

1.4.3 Moving Input Frequency-Constant Target Phase

Tracking a constant target phase with a moving input frequency is the second case in Fig. 1.8. In this test, the input frequency is modulated at 20 Hz. The input phase is then down sampled to 0.02 Hz oscillation. With the moving input, the controller is capable of settling the RF cavity to the new desired phase in 2 s within 0.3° of the target. The errors are slightly larger with the moving input frequency as the controller has to compensate for the slowly shifting input phase.

1.4.4 Constant Input Frequency-Moving Target Phase

Tracking a moving target with a constant input frequency is shown in Fig. 1.9. In this test the target phase modulates at varying frequencies between 90 and 100° while the input frequency remains constant. With this test the actual phase lags behind the target phase due to the nature of a feedback only controller. A feed forward controller or a controller that operates significantly faster than the phase oscillation could compensate for the phase lag between target and actual phase.

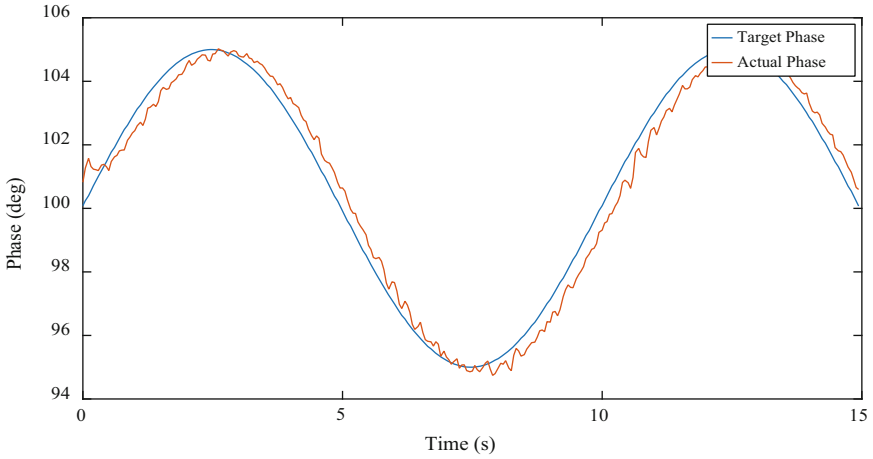

Fig. 1.10 Moving input frequency-moving target phase 0.1 Hz

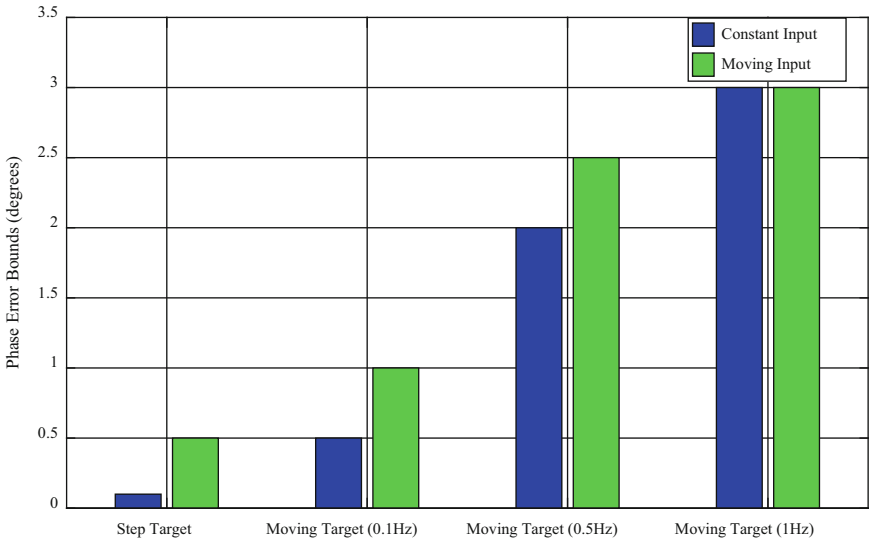

Fig. 1.11 Steady state phase error bounds

1.4.5 Moving Input Frequency-Moving Target Phase

Tracking a moving target phase while having a moving input frequency is the worst case scenario for RF cavity operation. In Fig. 1.10, the target phase oscillates between 90 and 100° at 0.1Hz and the input frequency also modulates. Even through this worst case scenario, the error bounds are $\pm 1°$ of the target largely due to system lag.

1.4.6 Steady State Error Comparison

Steady state error for the different test cases is shown in Fig. 1.11. As expected the fastest oscillating moving target causes the largest phase error, while the constant target cases result in the smallest. After accounting for demodulator error bounds, the constant target-constant input case is nearly within the desired error bounds for accelerator operation with a controller only operating at 20 Hz. A faster controller and higher quality demodulator would improve the response characteristics. The controller described is capable of tracking a moving target with reasonable fidelity as long as the moving target is not oscillating quickly.

1.5 Conclusions

Fast phase shifting of RF signals is possible using RF cavities as phase modulating devices. These cavities shift the phase of the incoming RF signal by modifying the resonance frequency of the cavity with respect to the input frequency. The shift in frequency is accomplished through piezo actuation of the cavity walls. A possible limitation of this approach, is the large losses experienced when coupling through an RF cavity. By controlling the input phase into each accelerating cavity in a bank individually, the overall efficiency of the accelerator can be increased yielding higher particle energies. Individual phase control will enable next generation particle accelerators like the MaRIE at Los Alamos National Lab to achieve unprecedented acceleration gradients and energy efficiency.

Acknowledgements The authors would like to thank Tsuyoshi Tajima for lending the RF cavity and Mark Prokop for lending the RF measurement equipment used for this study. We would also like to thank Lawrence Castellano and Phil Torrez for their help in setting up the RF experiment.

References

1. Ayvazyan, V., Simrock, S.: Dynamic Lorentz force detuning studies in Tesla cavities. In: Proceedings of European particle accelerator conference, Lucerne (2004)
2. Grecki, M., Andryszczak, J., Pozniak, T., Przygoda, K., Sekalski, P.: Compensation of Lorentz force detuning. In: Proceedings of EPAC08, Genoa (2008)
3. Kumar, A., Jana, A., Kumar, V.: A study of dynamic Lorentz force detuning of 650 MHz $\beta g{=}0.9$ superconducting radiofrequency cavity. Nucl. Instrum. Methods Phys. Res. Sect. A **750**, 69–77 (2014)
4. Liepe, M., Moeller, W., Simrock, S.: Dynamic Lorentz force compensation with a fast piezoelectric tuner. In: Proceedings of the 2001 Particle Accelerator Conference, Chicago (2001)
5. Simrock, S.: Lorentz force compensation of pulsed SRF cavities. In: Proceedings of LINAC2002, Gyeongju (2002)
6. Basak, S., Pandey, H., Chakrabarti, A.: Simulation analysis of analog IQ based LLRF control of RF cavity. In: Proceedings of PCaPAC2012, Kolkata (2012)

Chapter 2
Smart Setup and Accelerometer Mounting Check for Vibration Measurements

Bin Liu, Dmitri Tcherniak, Niels-Jørgen Jacobsen, and Martin Qvist Olsen

Abstract This paper describes some of the challenges experienced by many experimentalists and presents new ways of overcoming these. The Smart Setup can dramatically reduce the time required for the test setup and the presented Accelerometer Mounting Check procedure can check the transducer's health and the integrity of the whole measurement channel. The goal is to get the data right first time and in the shortest possible time.

Keywords Vibration measurement • Smart setup • System verification • Transducer mounting

2.1 Introduction

Performing vibration measurements can be quite time-consuming. In particular, proper mounting of transducers on the test structure, connecting them to the measurement hardware and checking everything is working as expected can be a significant part of the total test time. In addition, this often has to be done under extreme time constraints.

Obviously, not only large scale testing like modal surveys with hundreds of channels, but also smaller scaled tests, can benefit greatly from efficient measurement setup and system verification tools. Ensuring the integrity of each measurement channel becomes even more critical and difficult when transducers are located in remote areas or areas with limited or no access.

This paper first presents the technical background and the implementation of the patented technology called Accelerometer Mounting Check that can secure the health of all channels before and during measurements. Then Smart Setup, the patent-pending technology that can reduce measurement setup time, is introduced. A vibration measurement setup is used to illustrate the entire workflow.

2.2 Technical Background

Typical designs of piezoelectric accelerometer are shown in Fig. 2.1. They all have a similar mechanical principal: the active part of such an accelerometer is one or several piezoelectric elements that together, act as a spring connecting the base of the accelerometer to the seismic mass. When the base is mounted on a test object, its vibrations are transmitted via the accelerometer mount to the base and further to the seismic mass. The force acting on the piezoelectric elements produces a charge proportional to the force acting on it and hence, the acceleration of the seismic mass. Over the operational frequency range, the seismic mass vibrates with the same magnitude and phase as the accelerometer base and the surface on which the accelerometer is mounted [1], and the charge output of the accelerometer correctly reflects the acceleration of the test object.

The direct piezoelectric effect utilized in the accelerometers is a reversible process, that is, the same piezoelectric material exhibits the reverse effect: responding to the applied electrical field, it generates an internal mechanical strain. Applied to the mechanical scheme implemented in the accelerometer, the reverse effect means that subjecting the piezoelectric element with an alternating electric field, one will generate an alternating force acting on the seismic mass and the base. This force will be transmitted via the accelerometer structure and the accelerometer mount to the test object.

B. Liu (✉) • D. Tcherniak • N.-J. Jacobsen • M.Q. Olsen
Brüel & Kjær Sound & Vibration Measurement A/S, Skodsborgvej 307, Nærum 2850, Denmark
e-mail: bin.liu@bksv.com; dmitri.tcherniak@bksv.com; niels-jorgen.jacobsen@bksv.com; martinqvist.olsen@bksv.com

E. Wee Sit (ed.), *Sensors and Instrumentation, Volume 5*, Conference Proceedings of the Society for Experimental Mechanics Series, DOI 10.1007/978-3-319-29859-7_2

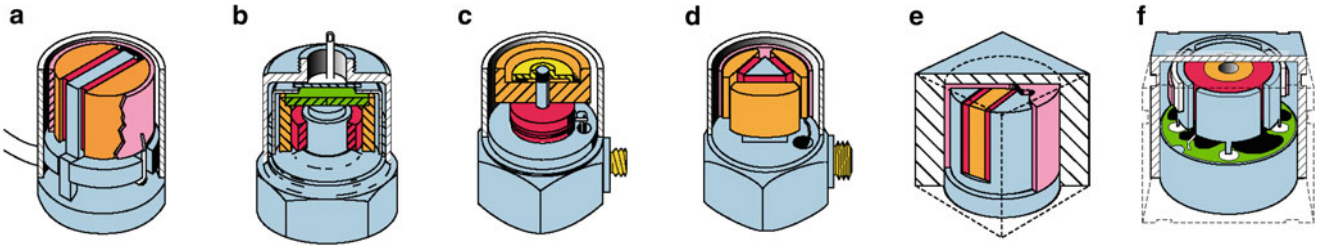

Fig. 2.1 Different designs of piezoelectric accelerometers: (**a**) PlanarShear; (**b**) annular shear; (**c**) centre-mounted compression; (**d**) DELTASHEAR®; (**e**) THETASHEAR®; (**f**) ORTHOSHEAR®

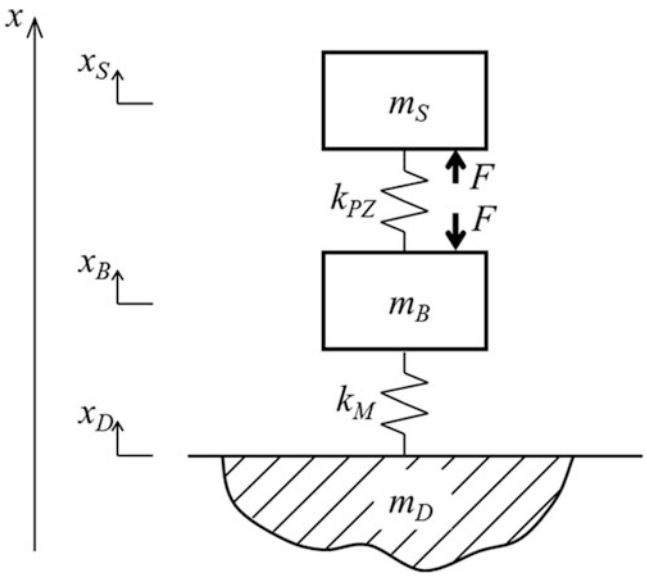

Fig. 2.2 Mechanical system representing the parts of the accelerometer and its mounting

If the accelerometer's output is measured simultaneously with applying the excitation voltage, one can notice that the readings are sensitive to the implementation of the accelerometer mount. This sensitivity is utilized in the Accelerometer Mounting Check technology.

Let us demonstrate the mechanical concept behind the Mounting Check on a simple model. The mechanical parts of the accelerometer, the mount and the test object are modelled as a three degree-of-freedom system (Fig. 2.2). The seismic mass and the accelerometer body, represented by masses m_S and m_B respectively, are connected by the piezoelectric element represented by a spring with linear stiffness k_{PZ}. The mount is modelled as the second linear spring with stiffness k_M, attached to the test object. Mass m_D models the part of the structure, which is involved in the local mechanical vibration of the accelerometer-structure assembly. The forces caused by applying the electric excitation to the piezoelectric element are denoted as F. By varying the parameters, one can observe how the accelerometer mounting (or the absence of mounting) affects the output of the accelerometer.

The equations of motion can be readily set

$$\begin{pmatrix} m_S & 0 & 0 \\ 0 & m_B & 0 \\ 0 & 0 & m_D \end{pmatrix} \begin{pmatrix} \ddot{x}_S \\ \ddot{x}_B \\ \ddot{x}_D \end{pmatrix} + \begin{pmatrix} k_{PZ} & -k_{PZ} & 0 \\ -k_{PZ} & k_{PZ}+k_M & -k_M \\ 0 & -k_M & k_M \end{pmatrix} \begin{pmatrix} x_S \\ x_B \\ x_D \end{pmatrix} = \begin{pmatrix} F \\ -F \\ 0 \end{pmatrix} \tag{2.1}$$

Assuming harmonic excitation $F = F_0 e^{i\omega t}$ and steady state of the system, the equations of motion can be solved. The electric output of the accelerometer is proportional to the forces acting on the piezoelectric element, which are proportional to its deformation $s = x_S - x_B$. The latter can be presented in the form $s(t) = s_0(\omega) e^{i\omega t}$, $s_0 \in \mathbb{C}$, and the expression for the frequency response function (FRF) $H(\omega) = s_0(\omega)/F_0$ can be found analytically or evaluated numerically.